Electronic Supplementary Material (ESI) for New Journal of Chemistry.

Porous Supramolecular assemblies and functional properties of perhydroxylated cucurbit[6]uril and polyoxometallates

Xi Xia,[a] Wei Wei Ge, [b] Haiyong Chen,[a] Zhu Tao,[a] Yunqian Zhang*[a] Gang Wei*[c] and Kai Chen*[b]

[a.] *Key Laboratory of Macrocyclic and Supramolecular Chemistry of Guizhou Province, Guizhou University, Guiyang 550025, China*
E-mail: sci.yqzhang@gzu.edu.cn (Yun-Qian Zhang)

[b.] *Collaborative Innovation Center of Atmospheric Environment and Equipment Technology, Jiangsu Key Laboratory of Atmospheric Environment Monitoring and Pollution Control, School of Environmental Science and Engineering, Nanjing University of Information Science & Technology, Nanjing 210044. E-mail: kaichen85@nuist.edu.cn or catqchen@163.com*

[c.] *CSIRO Manufacturing Flagship, PO Box 218, Lindfield, NSW 2070, Australia.E-mail: Gang.Wei@csiro.au.*

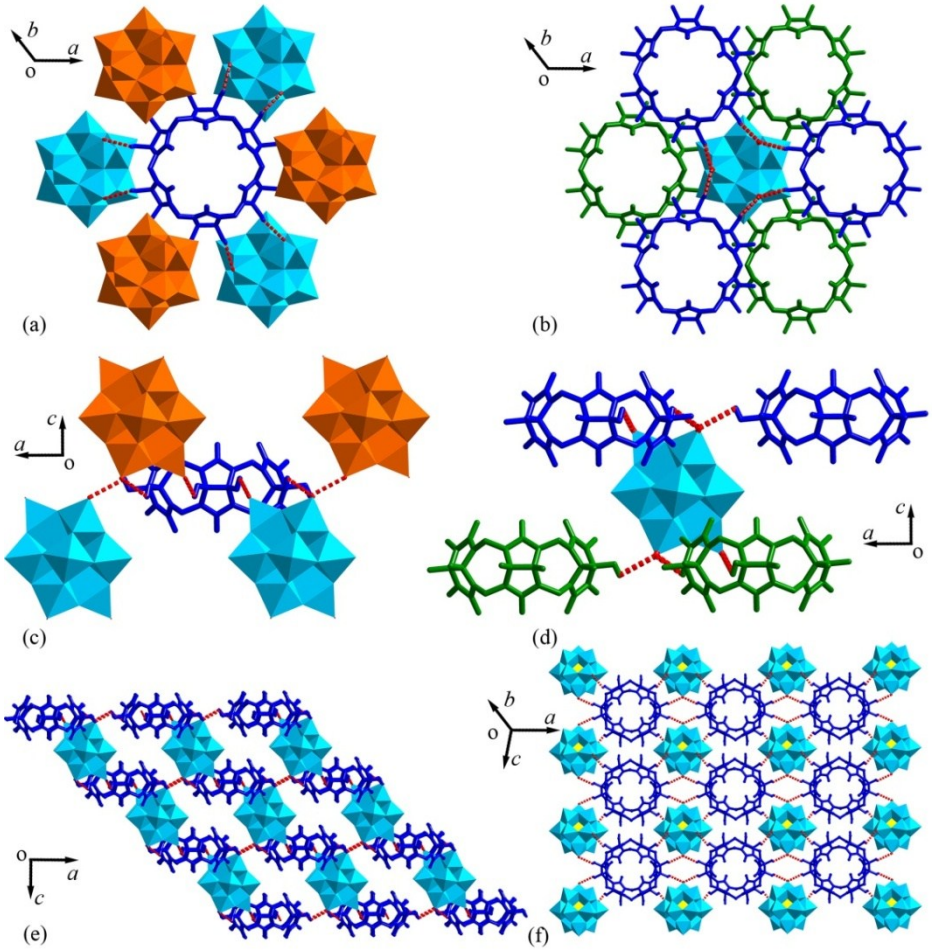

Fig. S1. Crystal structure of another **A**: (a and c) top view and side view of the detailed interactions of each $(HO)_{12}Q[6]$ molecule with six $[PWO_{40}]^{3-}$ anions; (b and d) top view and side view of the detailed interactions of each $[PWO_{40}]^{3-}$ anion with six $(HO)_{12}Q[6]$ molecules; (e) overview of the supramolecular stacking of $(HO)_{12}Q[6]$ molecules and $[PWO_{40}]^{3-}$ anions along *a* and *b* axes; (f) step-like supramolecular network of $(HO)_{12}Q[6]$ molecules and $[PWO_{40}]^{3-}$ anions along the *c* axes.

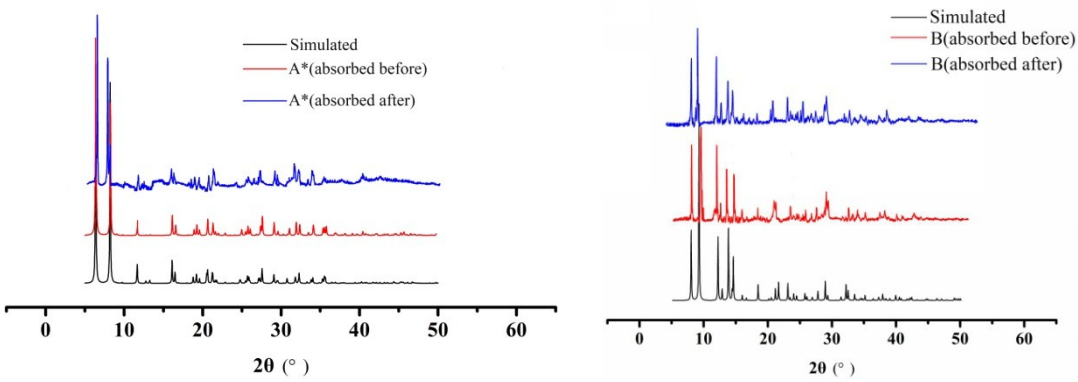

Fig. S2. Powder X-ray diffraction analysis of A* and B accompanied by simulations.

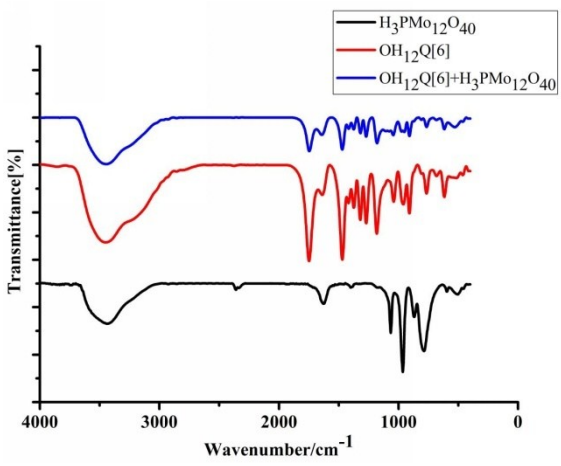

Fig. S3. FTIR spectra of $(HO)_{12}Q[6]$, $[PMo_{12}O_{40}]^{3-}$, hybrid of $(HO)_{12}Q[6]$ with $[PMo_{12}O_{40}]^{3-}$ anions

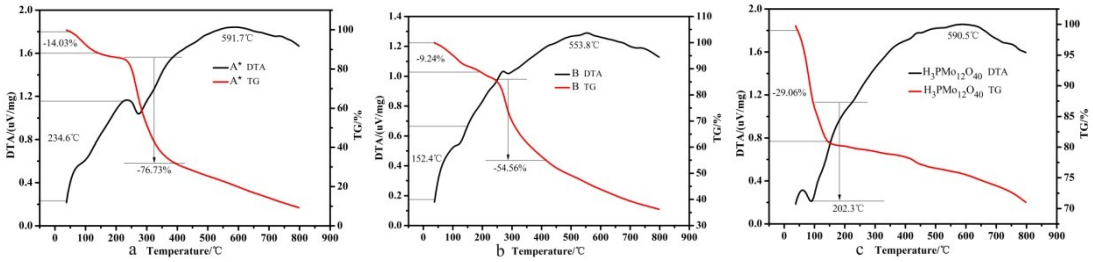

Fig. S4. DTA and TG profiles of (a) A*; (b) B; (c) $H_3PMo_{12}O_{40}$.

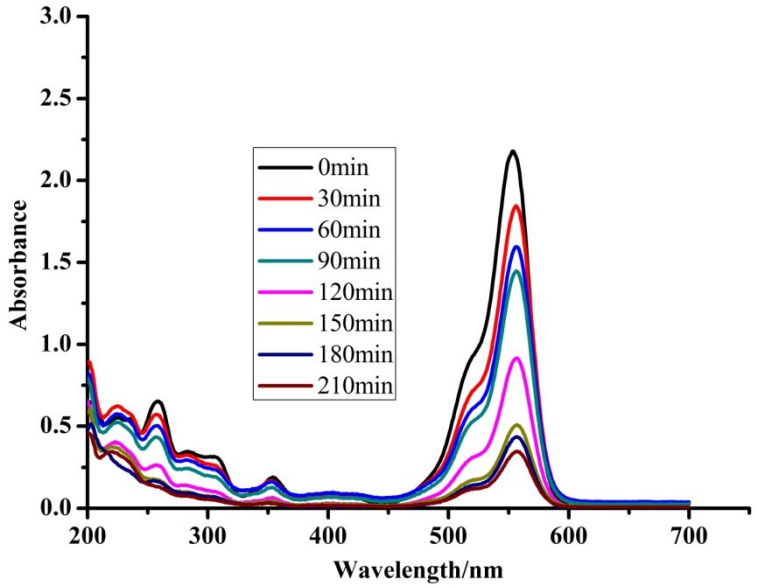

Fig. S5. Time-dependent UV/vis spectral changes of the rhodamine B solution in the presence of **A*** under visible light irradiation.

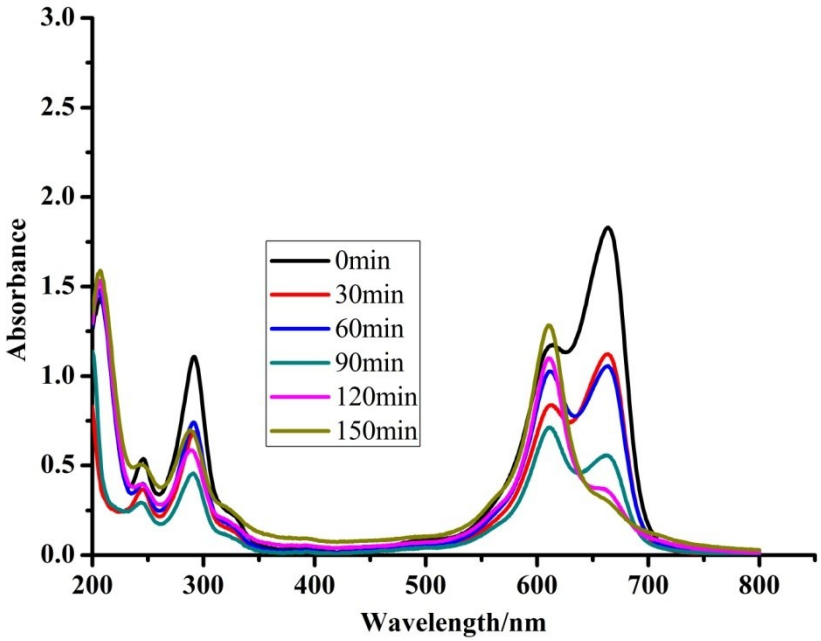

Fig. S6. Time-dependent UV/vis spectral changes of the acriflavine solution in the presence of **A*** under visible light irradiation.

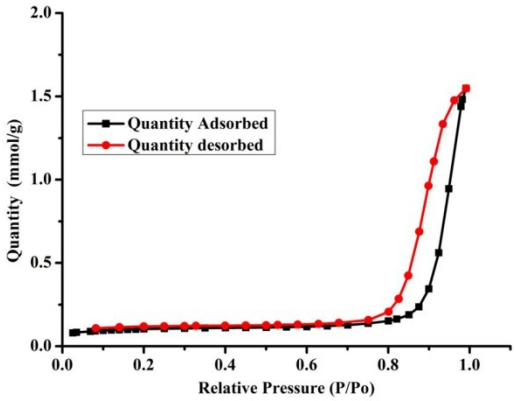

Fig.S7 The sorption isotherms of N_2 at 77 K by a micrometrics ASAP2020HD88 automated Adsorption analyser. ■ symbol = adsorption and, ● symbol = desorption of **A***.

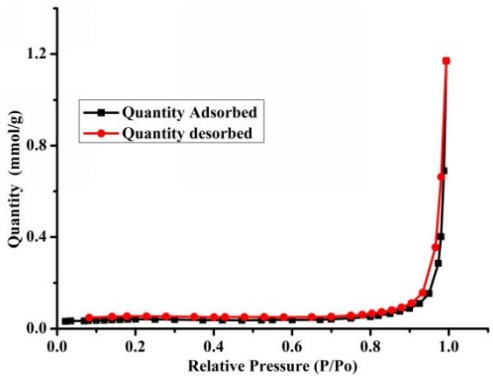

Fig. S8 The sorption isotherms of N_2 at 77 K by a micrometrics ASAP2020HD88 automated Adsorption analyser. ■ symbol = adsorption and, ● symbol = desorption of **B**.

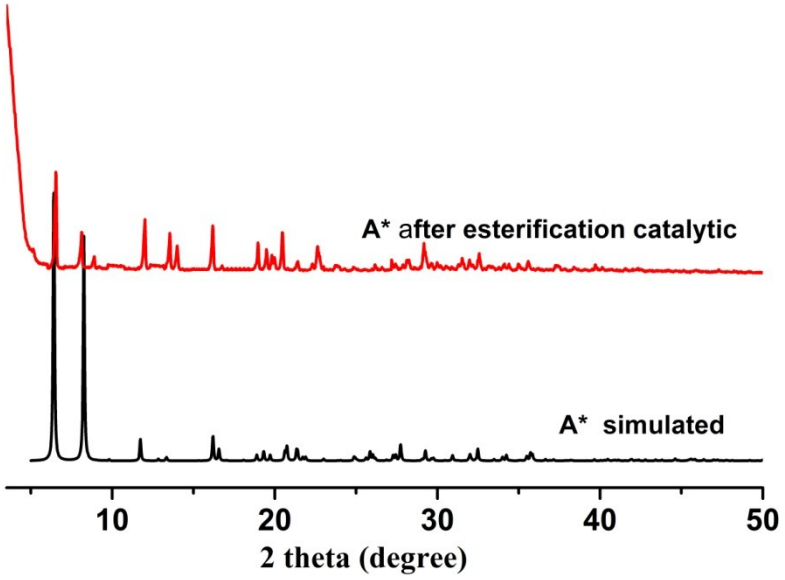

Fig. S9 Powder X-ray diffraction analysis of **A***: simulated and after etherification catalytic.

Table S1. Normalized adsorption data of **A*** and **B** for the selected volatile compounds ($g \cdot g^{-1}$)

Volatiles	**A***	**B**
tetrachloromethane	0.23	0.08
trichloromethane	0.38	0.20
dichloromethane	0.26	0.08
acetonitrile	0.12	0.09
ethoxyethane	0.14	0.07
ethanol	0.11	0.09
acetone	0.22	0.33
methanol	0.18	0.28

Table S2 Crystallographic data for compounds **A*, A** and **B**

Complex	**A***	**A**	**B**
empirical formula	$C_{36}H_{119}N_{24}O_{104}PMo_{12}$	$C_{36}H_{161}N_{24}O_{125}PW_{12}$	$C_{36}H_{77}N_{24}O_{43}Cl_3$
formula weight	3734.80	5168.06	1640.57
crystal system	hexagonal	hexagonal	hexagonal
space group	R -3m	R -3	R -3c
a (Å)	18.0014(11)	18.096(5)	22.317(3)
b (Å)	18.0014(11)	18.096(5)	22.317(3)
c (Å)	29.4043(18)	29.247(9)	22.272(3)
α (°)	90	90.00	90.00
β (°)	90	90.00	90.00
γ (°)	120	120.00	120.00
V ($Å^3$)	8251.9	8294(4)	9606(2)
Z	3	3	6
Dcalcd ($g \cdot cm^{-3}$)	2.255	3.104	1.701

μ(MoKα) (mm^{-1})	1.481	1.47	0.273
T (K)	293(2)	293(2)	293(2)
Unique reflns	1991	4426	2677
Obsdreflns	1678	3410	1881
Params	122	213	133
R_{int}	0.0663	0.0588	0.0608
R [I > 2σ(I)][a]	0.0755	0.0502	0.0712
*w*R[I>2σ(I)][b]	0.1657	0.1406	0.2209
R [all data][a]	0.0867	0.0694	0.0913
*w*R [all data][b]	0.1721	0.1494	0.2355
GOF on F^2	1.087	1.064	1.129

[a] $R_1 = \Sigma||F_o| - |F_c||/\Sigma|F_o|$. [b] $wR_2 = |\Sigma w(|F_o|^2 - |F_c|^2)|/\Sigma|w(F_o)^2|^{1/2}$, where $w = 1/[^2(F_o^2) + (aP)^2 + bP]$; $P = (F_o^2 + 2F_c^2)/3$.